Sub-10 nm Fe_3O_4@$Cu_{2-x}S$ Core-shell Nanoparticles for Dual-modal Imaging and Photothermal Therapy

Qiwei Tian, Junqing Hu, Yihan Zhu, Rujia Zou, Zhigang Chen, Shiping Yang, Runwei Li, Qianqian Su, Yu Han, and Xiaogang Liu**

Supporting Information

Characterizations: X-ray diffraction measurements were performed on a Bruker D4 X-ray diffractometer using Cu Kα radiation (λ = 0.15418 nm). The particle size, morphology, and microstructure of the Fe_3O_4@$Cu_{2-x}S$ core-shell nanoparticles were determined by a transmission electron microscope (JEM-2010F) and a field emission scanning electron microscope (S-4800). High-resolution scanning transmission electron microscopy (STEM) and energy-dispersive X-ray spectroscopy (EDS) were performed on an FEI Titan S-Twin transmission electron microscope operated at 300 kV. In a typical experiment, high-resolution STEM imaging was conducted with 70 μm C2 aperture, spot size 9, a high-angle annular dark-filed (HAADF) detector with inner detection angle larger than 76 mrad, and 100 mm camera length to ensure Z-contrast. Under such conditions, a spatial resolution of ~1.4 Å was obtained. EDS spectra and line scan were collected with 150 μm C2 aperture, spot size 6, and 60 s collection time. Fourier transform infrared spectra were recorded using KBr-pressed pellets on an IRPRESTIGE-21 spectrometer (Shimadzu). Ultraviolet-visible-near-infrared (UV-VIS-NIR) absorption spectra were measured on a LAMBDA 950 UV-VIS-NIR spectrophotometer using quartz cuvettes with an optical path of 1 cm. Contents of copper iron and iron ion in the solution were

determined by a Leeman Labs Prodigy high-dispersion inductively coupled plasma atomic emission spectroscopy (ICP-AES). The magnetic properties (M-H curve) were evaluated on a BHV-55 vibrating sample magnetometer. Magnetic resonance relaxometry was performed using a NMI20-Analyst NMR Analyzing & Imaging system (Shanghai Niumag Corporation).

Cytotoxicity assay: The *in vitro* cytotoxicity was measured using the methyl thiazolyl tetrazolium (MTT) assay in HeLa cells derived from human cervical carcinoma cell line.[1] Cells growing in a log phase were seeded into 96-well cell-culture plate (5×10^4/well) at 37 °C in DMEM (Dulbecco's Modified Eagle's Medium, which contains 10% fetal bovin serum, 4 mM glutamine, 100 U/ml penicillin, 100 mg/mL streptomycin and 1% hydroxyethyl piperazine ethanesulfonic acid) and in the presence of 5% CO_2 for 12 hours. The cells were then incubated with polymer-modified Fe_3O_4@$Cu_{2-x}S$ nanoparticles with varied Cu concentrations (i.e., 0, 13, 25, 50, 100, 200 and 400 ppm, diluted in DMEM) at 37 °C for 12 hours in the presence of 5% CO_2. Subsequently, 10 μL of MTT (5 mg/mL) was added to each well of the 96-well assay plate and incubated for another 4 hours at 37 °C in the presence of 5% CO_2. After the addition of 10% sodium dodecyl sulfate (SDS, 100 mL/well), the assay plate was allowed to stand at room temperature for 12 hours. Multiskan MK3 monochromator-based multifunction microplate reader was used to measure the absorbance of each well with background subtraction at 492 nm. The tests were independently performed for three times.

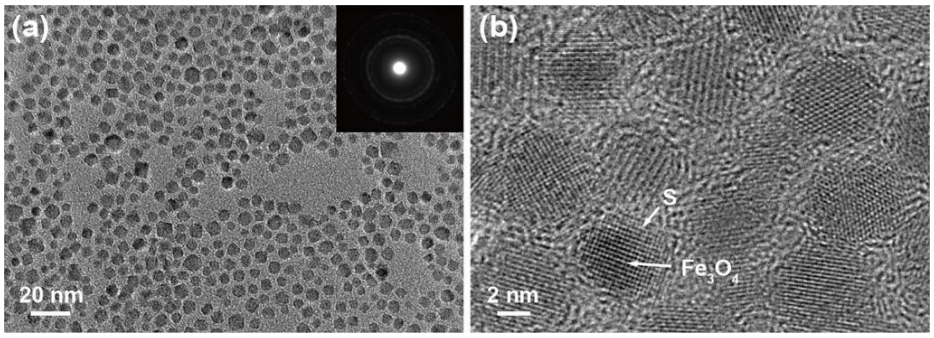

Figure S1. (a) Low-magnification TEM image (inset: corresponding electron diffraction pattern) of the as-synthesized Fe_3O_4@S nanoparticles and (b) high-magnification TEM image of the Fe_3O_4@S nanoparticles.

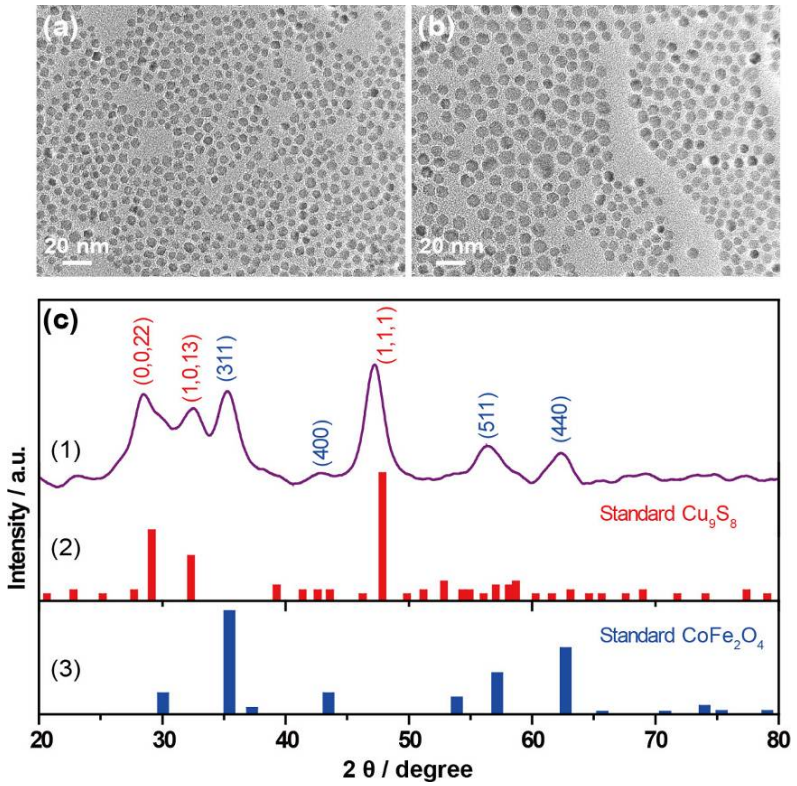

Figure S2. (a, b) TEM images of the starting $CoFe_2O_4$ nanoparticles (a) and the as-synthesized $CoFe_2O_4$@$Cu_{2-x}S$ core-shell nanoparticles (b). (c) Powder XRD patterns of the $CoFe_2O_4$@$Cu_{2-x}S$ nanoparticles as referenced by standard Cu_9S_8 (JCPDS file number: 36-0379) and $CoFe_2O_4$ (JCPDS file number: 03-0864) phases.

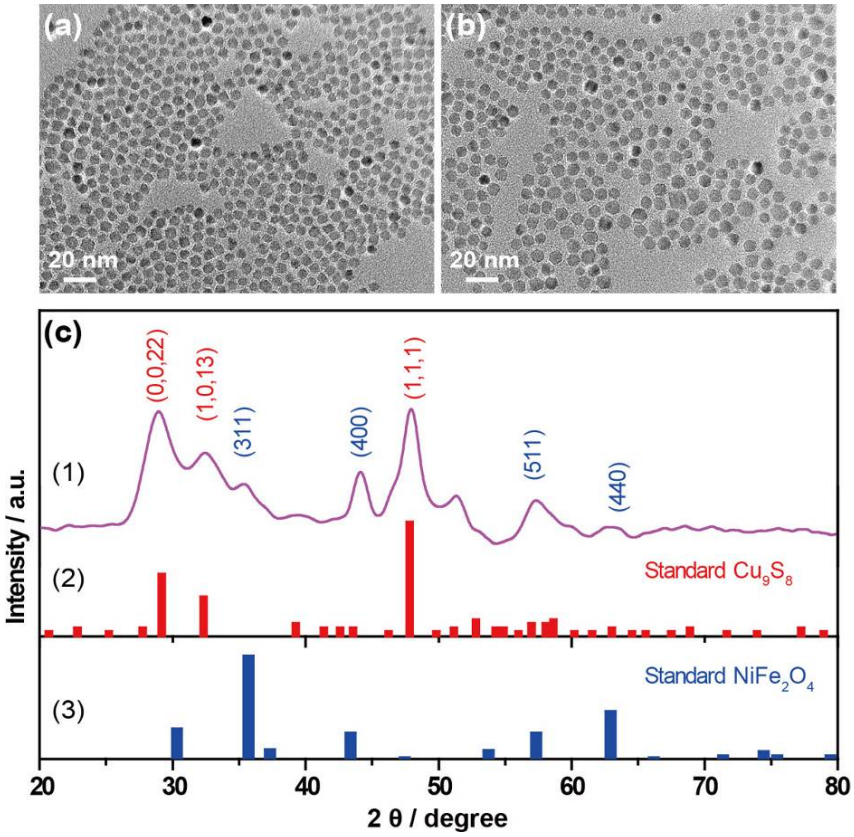

Figure S3. (a, b) TEM images of the starting $NiFe_2O_4$ nanoparticles (a) and the as-synthesized $NiFe_2O_4$@$Cu_{2-x}S$ core-shell nanoparticles (b). (c) Powder XRD patterns of the $NiFe_2O_4$@$Cu_{2-x}S$ core-shell nanoparticles as referenced by standard Cu_9S_8 (JCPDS file number: 36-0379) and $NiFe_2O_4$ (JCPDS file number: 54-0964).

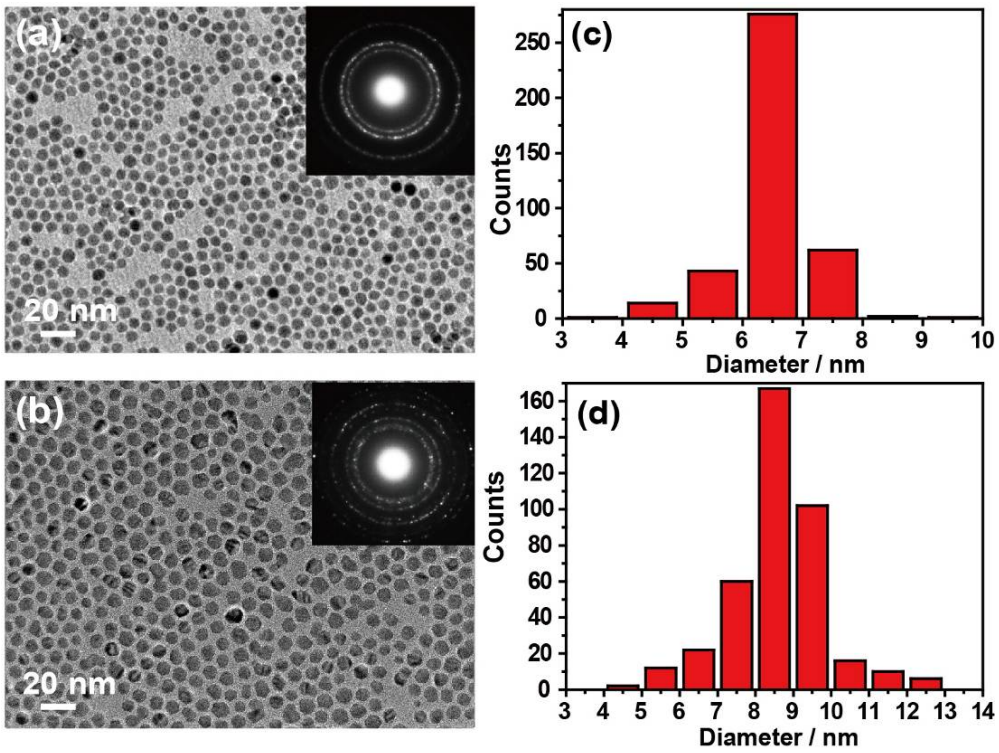

Figure S4. (a,b) TEM images of the as-obtained Fe_3O_4 and $Fe_3O_4@Cu_{2-x}S$ nanoparticles, respectively (inset: corresponding ED patterns). (c,d) Corresponding particle size distributions of the Fe_3O_4 and $Fe_3O_4@Cu_{2-x}S$ nanoparticles, respectively. The size distributions were obtained by measuring ~ 400 particles.

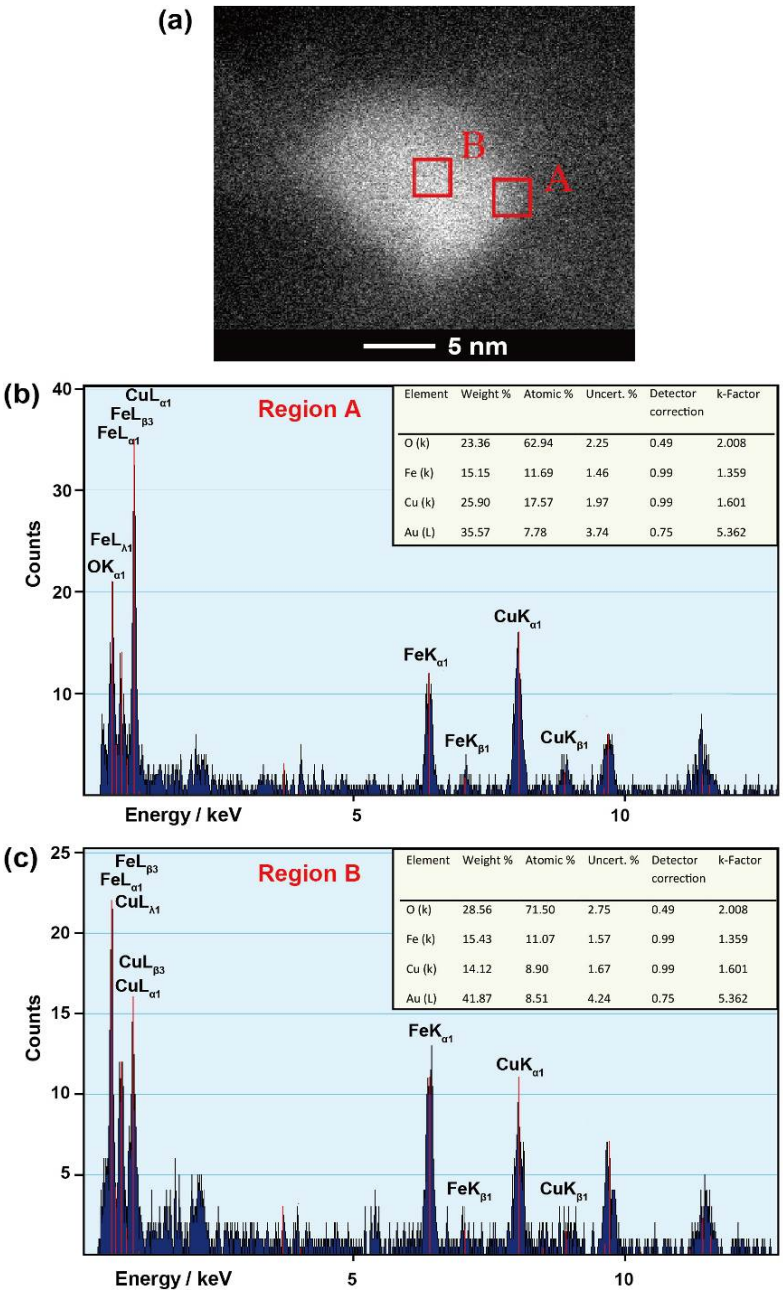

Figure S5. (a) STEM image of a single Fe_3O_4@$Cu_{2-x}S$ nanoparticle with the periphery and center regions of EDX signal acquisition marked as **A** and **B**, respectively. (b, c) EDX spectra taken for the regions of **A** and **B**, respectively (Insets: compositional analysis of regions **A** and **B**). The EDX spectra and the quantitative elemental mapping of the nanoparticle suggest that region **A** contains more Cu while region **B** contains more Fe. Note that the aforementioned EDX analysis was conducted on a gold (Au) TEM grid instead of commonly used Cu grid, in order to acquire accurate information of Cu in the sample. The attempt to undertaking an EDX elemental mapping on the whole particle was unsuccessful as prolonged electron beam irradiation caused severe specimen contamination, possibly due to the generation of elemental sulfur from the sample.

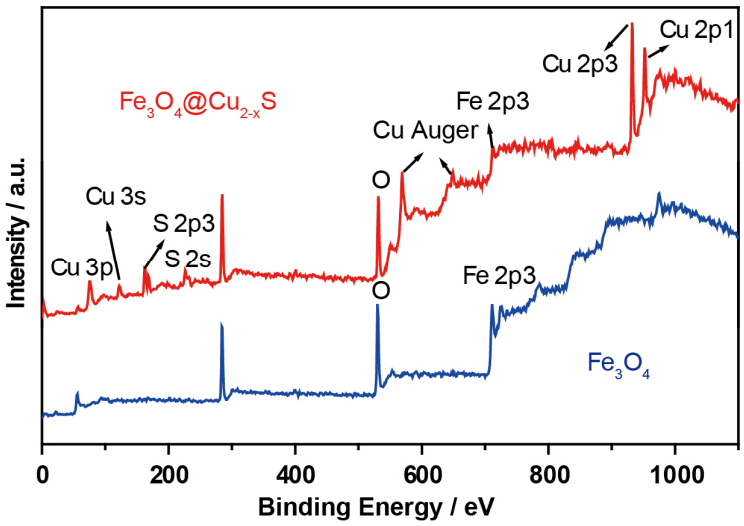

Figure S6. X-ray photoelectron spectroscopy spectra of the Fe_3O_4 nanocrystals (blue line) and the as-synthesized $Fe_3O_4@Cu_{2-x}S$ core-shell nanoparticles (red line).

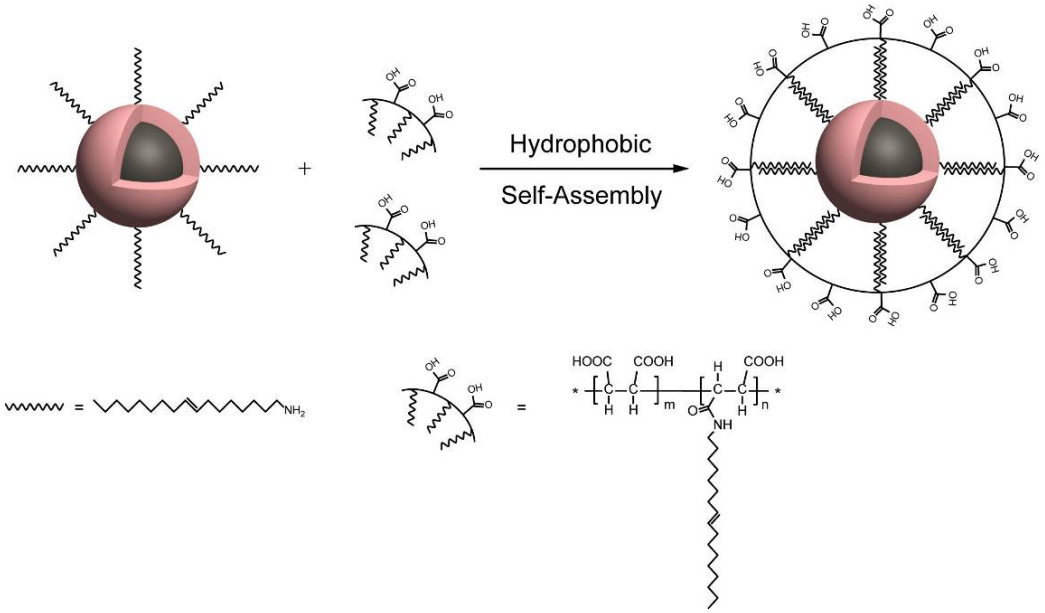

Figure S7. Schematic presentation showing the synthetic procedure for hydrophilic $Fe_3O_4@Cu_{2-x}S$ core-shell nanoparticles.

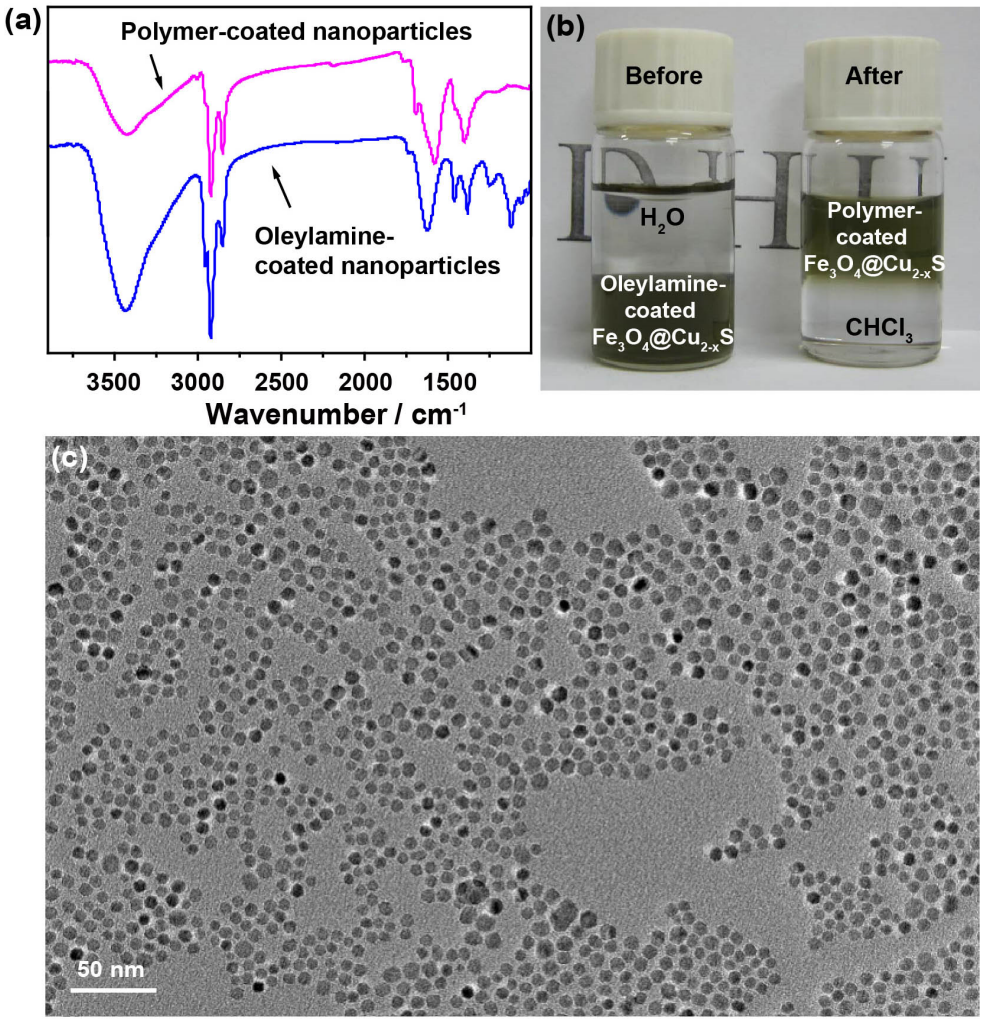

Figure S8. (a) FTIR spectra of the $Fe_3O_4@Cu_{2-x}S$ nanoparticles before (blue line) and after (magenta line) polymer coating. The broad band centered around 3450 cm^{-1} corresponds to N-H and/or O-H stretching vibration.[2] The two bands at 2924 and 2854 cm^{-1} are assigned to the asymmetric (ν_{as}) and symmetric (ν_{s}) stretching vibrations of methylene (CH_2) in the long alkyl chain, respectively. In addition, two bands at 1634 and 1384 cm^{-1} are attributed to N-H bending and C-N stretching modes, respectively.[1,3] The polymer coating was confirmed by the presence of a strong peak at 1700 cm^{-1} due to C = O stretching vibration of acid amides and two peaks at 1580 and 1400 cm^{-1} assigned to antisymmetric and symmetric vibration modes of $–COO^-$, respectively. (b) A digital camera photo showing the dispersion of the oleylamine- and polymer-coated $Fe_3O_4@Cu_{2-x}S$ nanoparticles in water and chloroform, respectively. (c) TEM image of the corresponding hydrophilic $Fe_3O_4@Cu_{2-x}S$ nanoparticles.

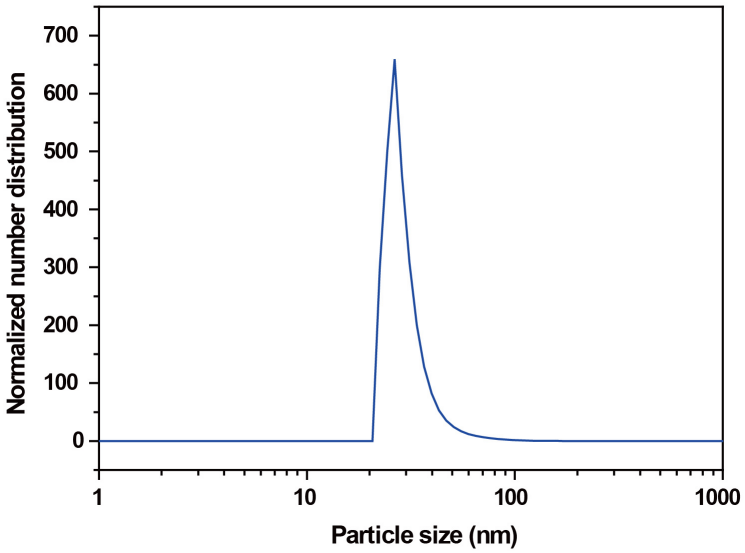

Figure S9. Dynamic light scattering (DLS) analysis of the polymer-coated $Fe_3O_4@Cu_{2-x}S$ nanoparticles. The DLS result indicates a particle size of about 26 nm, which is larger than that obtained by TEM. Note that the DLS technique measures the hydrodynamic size of the $Fe_3O_4@Cu_{2-x}S$ nanoparticles surrounded by the polymer layer.[4]

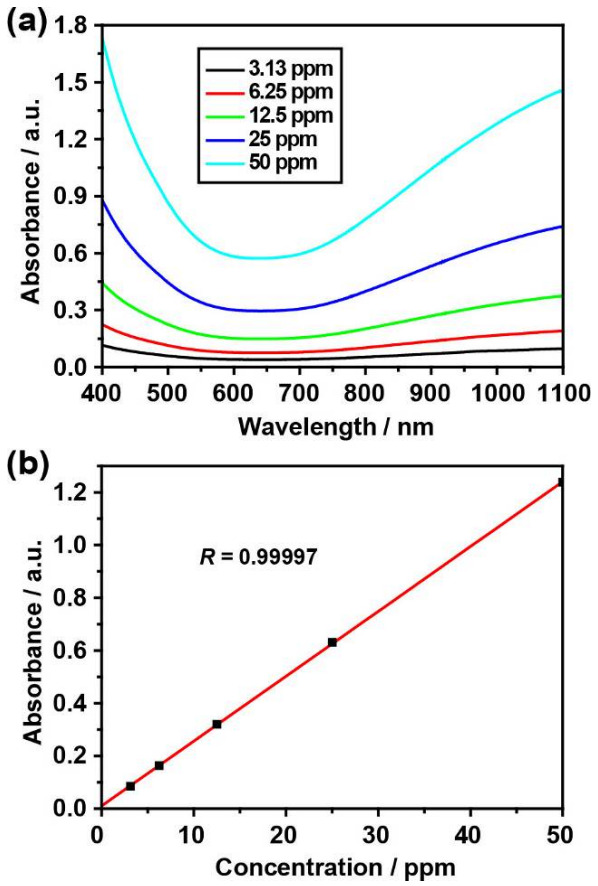

Figure S10. (a) Room temperature UV-VIS-NIR absorbance spectra for the $Fe_3O_4@Cu_{2-x}S$ core-shell nanoparticles dispersed in water with various solution concentrations of Cu. (b) Plots of linear fitting extinction versus wavelength for the solutions of the $Fe_3O_4@Cu_{2-x}S$ core-shell nanoparticles at 980 nm.

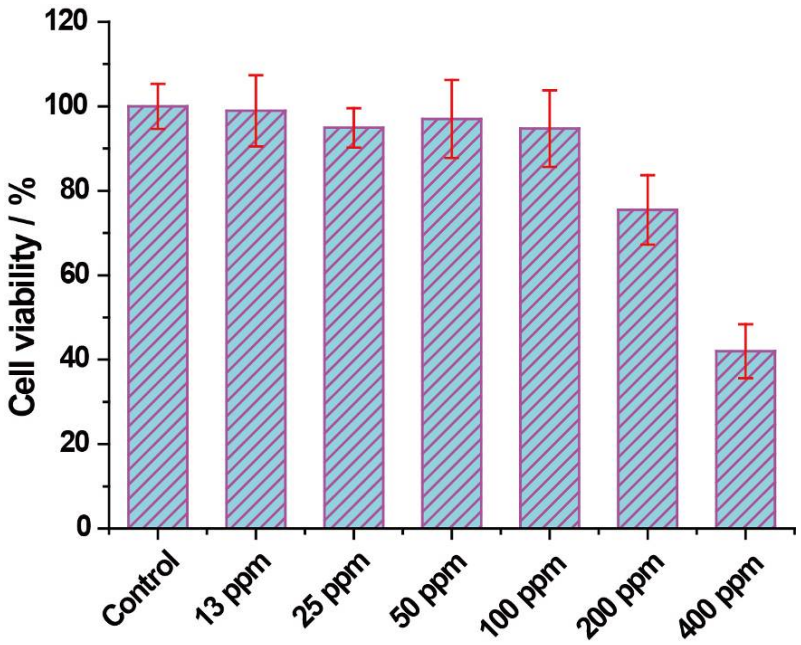

Figure S11. Cell viabilities estimated by the MTT proliferation test versus incubation concentration (0-400 ppm) of polymer-modified Fe_3O_4@$Cu_{2-x}S$ nanoparticles. The cells were incubated in solutions of the polymer-modified core-shell nanoparticles at 37 °C for 12 hours in the presence of 5% CO_2. The cell toxicity testing results show that marked difference in the proliferation of the cells was observed in the presence of the polymer-modified nanoparticles with Cu concentrations of 0-100 ppm, and the cellular viability was estimated to be higher than 80% after 12 h incubation. Therefore, it is believed that the solution of the polymer-modified nanoparticles with a low Cu concentration (< 100 ppm) is considered to have a relatively low cytotoxicity.

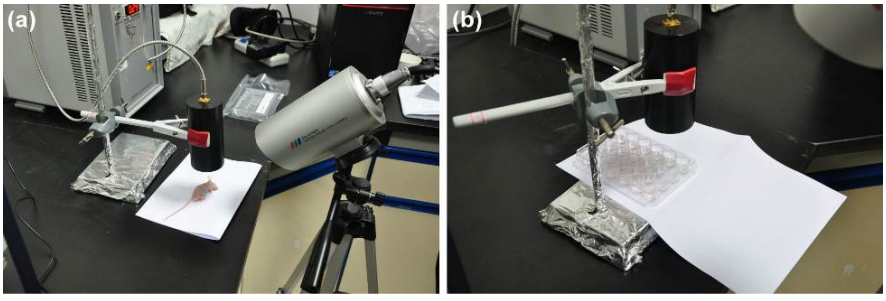

Figure S12. Photographs showing the typical experimental setup for (a) *in vivo* infrared thermal imaging study with the Fe_3O_4@$Cu_{2-x}S$ core-shell nanoparticles and photothermal ablation of HeLa cells using the core-shell nanoparticles.

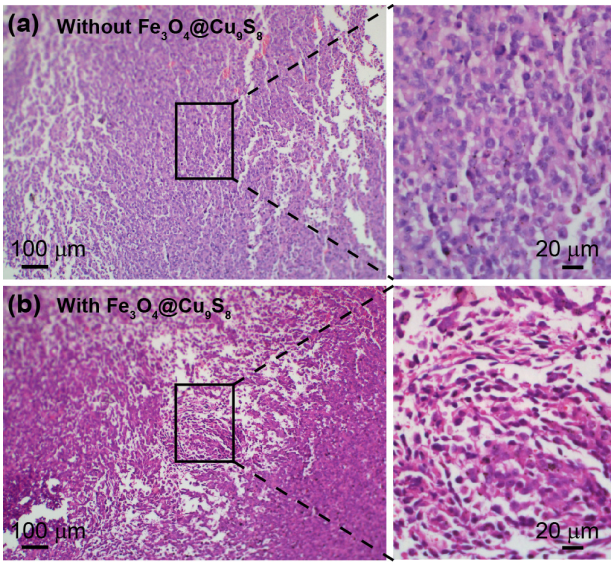

Figure S13 Representative H & E stained histological images of *ex vivo* tumor sections injected with: (a) water only and (b) an aqueous dispersion of polymer-modified $Fe_3O_4@Cu_{2-x}S$ nanoparticles (Cu content: 50 ppm), respectively. The sections were irradiated with the 980-nm laser irradiation for 10 min. Note that the power density used is 0.6 W/cm^2.

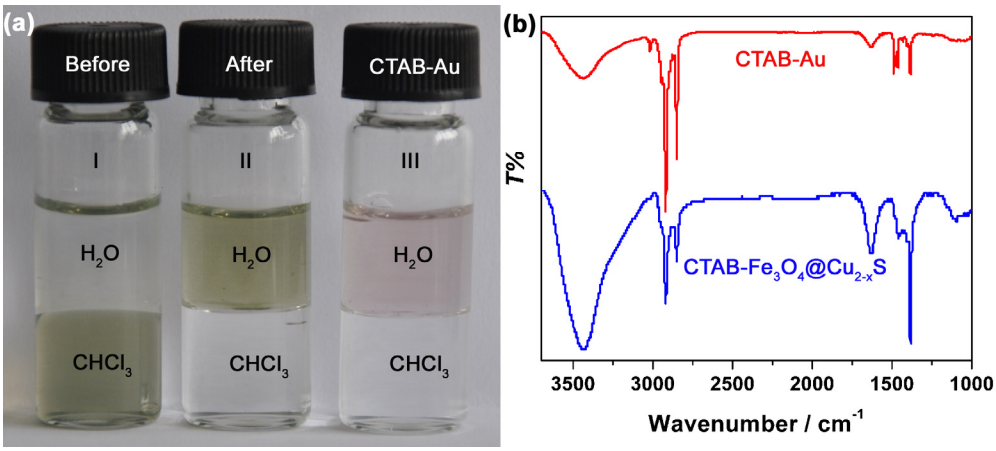

Figure S14 (a) Stability test of the $Fe_3O_4@Cu_{2-x}S$ nanoparticles (I and II) before and after being modified with CTAB and the as-prepared CTAB-capped Au nanorods (III). (b) The FTIR spectra of the Au nanorods and $Fe_3O_4@Cu_{2-x}S$ nanoparticles modified with the CTAB.

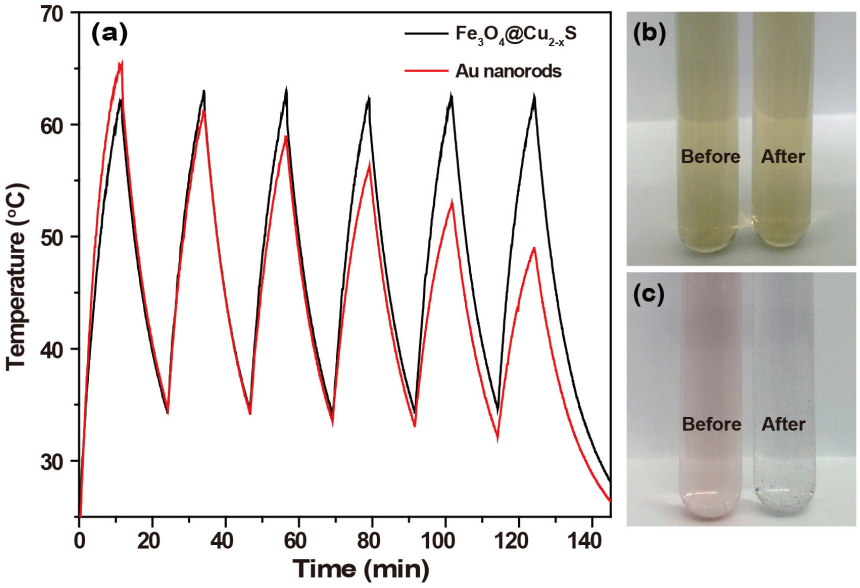

Figure S15. (a) Photothermal stability investigations of Fe_3O_4@$Cu_{2-x}S$ nanoparticles and Au nanorods by monitoring the solution temperature as a function of laser heating time. Note that the 980 nm laser was turned on and off for six repeated cycles. To rule out the polymer coating effect on the stability of the core-shell nanoparticles, we replaced the polymer coating with cetrimonium bromide (CTAB) stabilizing molecules through a hydrophobic self-assembly method.[5] (b, c) photographs of dispersions of the CTAB-coated Fe_3O_4@$Cu_{2-x}S$ nanoparticles and Au nanorods, respectively, in water before and after the laser heating treatment. We noticed an obvious color change in Au nanorod solution after six repeated cycles of laser heating.

References:

[1] X. M. Lu, H. Y. Tuan, J. Y. Chen, Z. Y. Li, B. A. Korgel, Y. N. Xia, *J. Am. Chem. Soc.* **2007**, *129*, 1733.

[2] M. Nakaya, M. Kanehara, T. Teranishi, *Langmuir* **2006**, *22*, 3485.

[3] W. B. Bu, Z. X. Chen, F. Chen, J. L. Shi, *J. Phys. Chem. C* **2009**, *113*, 12176.

[4] C. I. Olariu, H. H. P. Yiu, L. Bouffier, T. Nedjadi, E. Costello, S. R. Williams, C. M. Halloran, M. J. Rosseinsky, *J. Mater. Chem.* **2011**, 21, 1265.

[5] I. Gorelikov, N. Matsuura, *Nano Lett.* **2007**, 8, 369.